Available online at www.sciencedirect.com
SCIENCE DIRECT®
International Journal of Heat and Mass Transfer 48 (2005) 5047–5057
International Journal of HEAT and MASS TRANSFER
www.elsevier.com/locate/ijhmt

Analysis of thermal effects in a spherical adsorbent pellet

Krzysztof Kupiec [a,*], Andreas Georgiou [b]

[a] Cracow University of Technology, Institute of Chemical and Process Engineering, ul. Warszawska 24, 31-155 Cracow, Poland
[b] Frederick Institute of Technology, Filias Str. 1A, Limassol 3110, Cyprus

Available online 29 August 2005

Abstract

A new model of nonisothermal adsorption is presented. The model is applicable to systems with nonlinear adsorption isotherm. Both intraparticle and film mass-transfer resistances are accounted in the model with the intraparticle mass-transfer rate being controlled by pore diffusion. An analytical solution of the model equations has been developed and a criterium for the existence of a maximum in the temperature uptake curves has been presented. A simple algorithm for the calculation of the maximum particle temperature has been illustrated. A detailed sensitivity analysis has shown the influence of various parameters on the temperature uptake curves. The model has been applied to the system water vapour–alumina and the predicted temperature uptake curves were compared with experimental results.

Keywords: Intraparticle diffusion; Heat transfer; Heat of adsorption; Nonlinear isotherm; Mathematical models

1. Introduction

Adsorption processes are widely applied in such processes as water treatment, atmospheric pollution prevention and the separation and purification of products [1,2]. Pressure Swing Adsorption is applied in large scale industrial processes such as the production of bioethanol which is an important renewable fuel additive [3]. The modeling, simulation and optimization of large scale processes have important implications on their economics and industrial viability. The modeling requires information about the equilibrium, kinetics and dynamics of the process. Adsorption processes are in general exothermic. If the concentrations of the adsorbed components are high and the heat of adsorption significant, the heat effects cannot be neglected. In the case of trace systems, the processes may in general be considered isothermal. It is obvious that in many cases it is difficult to predict the significance of the heat effects. When the adsorption heat effect cannot be neglected, the models of the adsorption processes become more complicated. It is therefore very important to establish simple and accurate criteria which allow one to check the validity of the assumption of the process being isothermal.

During adsorption, heat is generated which partly is transferred to the surrounding fluid and partly is accumulated in the particle leading to a temperature increase. The calculation of the temperature uptake curves is based on mathematical models of different complexity depending on the simplifying assumptions being made. The most widely applied simplifying assumptions are

1. The isotherm is linear. This assumption is particularly useful in the derivation of analytical solutions of the model equations [4–6]. In most practical systems however the isotherms are nonlinear making

* Corresponding author.
E-mail addresses: kkupiec@chemia.pk.edu.pl (K. Kupiec), geor-and@cytanet.com.cy (A. Georgiou).

0017-9310/$ - see front matter © 2005 Elsevier Ltd. All rights reserved.
doi:10.1016/j.ijheatmasstransfer.2005.06.013

Nomenclature

Bi	mass-Biot number
c_g	heat capacity of the fluid
c_p	heat capacity of the pellet
C_b	component concentration in the bulk
D_p	effective pore diffusion coefficient
E_0	constant in Eqs. (49) and (50)
h	heat transfer coefficient
ΔH	heat of adsorption
k_g	mass-transfer coefficient
K_0	constant in Eq. (49)
p	partial pressure
p_s	saturation pressure
Pr	Prandtl number
$\bar{q}_m$	average component concentration in the pellet, [kg/kg]
q_{mb}	component concentration in the pellet at equilibrium with C_b, [kg/kg]
R	gas constant (=8.314 J/mol K)
RH	relative humidity
R_p	radius of the pellet
Sc	Schmidt number
t	time
T	pellet temperature
T_0	initial temperature of the pellet
T_b	fluid temperature
ΔT_{ad}	adiabatic rise of temperature
u	fluid velocity
$\overline{Y}$	dimensionless average solid concentration

Greek symbols

β	constant (Eq. (10))
γ	constant (Eq. (11))
δ	constant defined by Eq. (14)
ζ	constant defined by Eq. (29)
η	constant defined by Eq. (35)
λ	adsorption equilibrium constant
ρ_g	fluid density
ρ_p	pellet density
ν	exponent in Freundlich equation
σ	constant defined by Eq. (30)
θ	dimensionless temperature
θ_b	constant defined by Eq. (31)
τ	dimensionless time
ψ	constant defined by Eq. (26)

these models inaccurate. The linearization of the isotherm leads to the underestimation of the intraparticle mass-transfer rate and consequently the predicted maximum particle temperature is smaller than the observed.

2. The external mass-transfer resistances are negligible. This assumption is rather controversial because at the initial stages of the process when the heat effects are most significant, the external mass-transfer resistances are usually rate controlling. As shown by Hills [7], this assumption leads to greater errors than the assumption that the isotherm is temperature independent.
3. The adsorption isotherm parameters are independent of temperature. As shown by Hills [7], in the case of small temperature rises (less than 10 K), the assumption that the isotherm is temperature independent does not lead to significant errors.
4. The diffusion coefficient, heat capacity and heat of sorption are independent of temperature.
5. The particle temperature gradients are negligible and the heat transfer resistance is contributed by the film surrounding the particle. As shown by Brunovska et al. [8] the lumped thermal model of nonisothermal adsorption is a very good approximation to the complete model for many practical systems.
6. The intraparticle mass-transfer rate can be approximated using driving force models. Bowen and Rimmer [9] applied Vermeulen's Quadratic Driving Force model [10] in the analysis of experimental results for the system water vapour–alumina. Bhaskar and Do [11] developed approximate models for nonisothermal adsorption with a linear isotherm using the parabolic (LDF model) and the nth order approximation of the intraparticle concentration profile.

Ruthven et al. [6] have assumed that the external mass-transfer resistances are negligible and the equilibrium relationships are linear i.e. $(\partial q_m/\partial T)_p = \text{const}$. The analytical solution for the temperature history is then

$$(T - T_0)\left(\frac{\partial q_m}{\partial T}\right)_p = q_{mb} \cdot \sum_{n=1}^{\infty} \frac{3[(p_n \cot p_n - 1)/p_n^2] \cdot \exp(-p_n^2 \tau)}{\frac{1}{\beta'} + \frac{3}{2} \cdot [p_n \cot p_n (p_n \cot p_n - 1)/p_n^2 + 1]} \quad (1)$$

where p_n are the roots of

$$3\beta'(p_n \cot p_n - 1) - p_n^2 + \alpha' = 0 \quad (2)$$

with the parameters α' and β' given by

$$\alpha' = \frac{h\lambda R_p}{D_p c_p} \quad (3)$$

$$\beta' = \frac{\Delta H}{c_p} \cdot \left(\frac{\partial q_m}{\partial T}\right)_p \quad (4)$$

A literature review shows that simple and accurate models for the case of nonisothermal adsorption with a nonlinear isotherm and mass-transfer resistances both in the film and in the particle are currently not available. In this work a new approximate model is developed for this particular case. The resulting equations are analytically integrated to obtain the time dependence of the particle temperature. A simple criterium for the existence of a maximum in the temperature uptake curve is developed and a simple algorithm for the calculation of the maximum particle temperature is illustrated. A detailed sensitivity analysis performed shows the influence of various parameters on the temperature uptake curves. The model is further applied to the system water vapour–alumina and the predicted temperature uptake curves were compared with the experimental results by Bowen and Rimmer [9].

2. Kinetic equation for Freundlich systems with macropore diffusion control

Currently a number of kinetic equations for nonlinear isotherm systems with macropore diffusion control is available [12–14]. In this work the kinetic equation developed by Kupiec [12] has been used to describe the mass-transfer rate. This kinetic equation is applicable to systems with both intraparticle and film mass-transfer resistances. Furthermore its simple form and accuracy allow the derivation of an analytically integrable mathematical model of nonisothermal adsorption process. In dimensionless form this kinetic equation is

$$\frac{d\overline{Y}}{d\tau} = \frac{3}{\beta\overline{Y} + \frac{\gamma}{Bi}} \tag{5}$$

where $\overline{Y}$ is the dimensionless volume averaged concentration in the particle:

$$\overline{Y} = \frac{\bar{q}_m}{q_{mb}} \tag{6}$$

The dimensionless time is defined as

$$\tau = \frac{D_p t}{\lambda R_p^2} \tag{7}$$

while the mass-Biot number is given by

$$Bi = \frac{k_g R_p}{D_p} \tag{8}$$

The adsorption equilibrium parameter λ is

$$\lambda = \frac{q_{mb}\rho_p}{C_b} \tag{9}$$

The parameters β and γ are linear functions of the Freundlich exponent:

$$\beta = 1/3 + 0.351v \tag{10}$$

$$\gamma = 1 + 0.143v \tag{11}$$

The kinetic equation (5) is limited to short times ($\overline{Y} < 0.5$). For the current analysis however this limitation is not important because the heat effects are most significant in the initial stages of the process.

Upon integration of Eq. (5) with the condition $\tau = 0$, $\overline{Y} = 0$ one obtains

$$\tau = \frac{1}{6}\left(\beta\overline{Y}^2 + \frac{2\gamma\overline{Y}}{Bi}\right) \tag{12}$$

and therefore for $\overline{Y} > 0$

$$\overline{Y} = \frac{\gamma}{\beta Bi}\left(\sqrt{1+\delta\tau} - 1\right) \tag{13}$$

where

$$\delta = \frac{6\beta Bi^2}{\gamma^2} \tag{14}$$

These formulas are applicable for $\tau < \tau_{max}$ where

$$\tau_{max} = \frac{1}{6}\left(\frac{\beta}{4} + \frac{\gamma}{Bi}\right) \tag{15}$$

resulting from Eq. (12) with $\overline{Y} = 0.5$. In Fig. 1 the dependence of τ_{max} on the Freundlich exponent for various values of the mass-Biot number is shown.

Eq. (5) is very accurate for all values of the Freundlich exponent and for all values of the mass-Biot number. An analysis of some particular cases is given below:

Rectangular isotherm. For $v = 0$ then $\beta = 1/3$ and $\gamma = 1$. Upon substitution to Eq. (12) one obtains:

$$\tau = \frac{1}{6}\left(\frac{1}{3}\overline{Y}^2 + \frac{2\overline{Y}}{Bi}\right) \tag{16}$$

In the case of a rectangular isotherm the exact analytical solution is [15]:

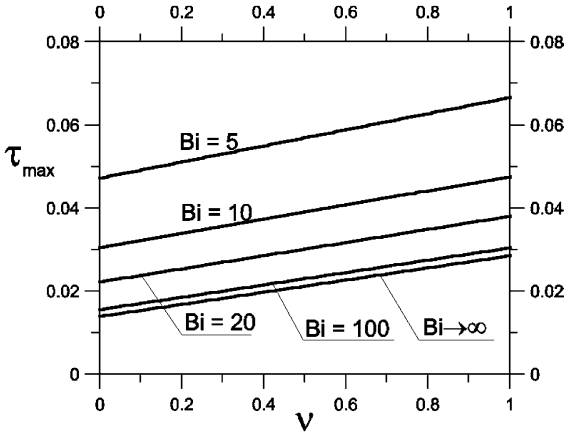

Fig. 1. Dependency of τ_{max} on Freundlich exponent v and the mass-Biot number Bi.

$$\tau = \frac{1}{6}\left[1 + 2(1-\overline{Y}) - 3(1-\overline{Y})^{2/3} + \frac{2\overline{Y}}{Bi}\right] \tag{17}$$

For small values of the fractional uptake, the above Eq. (17) can be simplified leading to Eq. (16). For extreme values of the mass-Biot number, Eq. (16) can be simplified to give well known kinetic equations as follows:

For $Bi \to 0$ one obtains

$$\overline{Y} = 3Bi \cdot \tau \tag{18}$$

while for $Bi \to \infty$ one obtains the following asymptotically exact formula [15]:

$$\overline{Y} = \sqrt{18\tau} \tag{19}$$

Linear isotherm. In this case the Freundlich exponent is $v = 1$. From Eqs. (10) and (11) the values $\beta = 0.684$ and $\gamma = 1.143$ can be obtained. Upon substitution to Eq. (13) one obtains:

$$\overline{Y} = \frac{3}{Bi} \cdot 0.557\left(\sqrt{1 + \pi Bi^2\tau} - 1\right) = \frac{3}{Bi} \cdot f_1\left(Bi\sqrt{\tau}\right) \tag{20}$$

For small values of the dimensionless time the particle can be treated as a semi-infinite medium and the following asymptotically exact equation for the fractional uptake can be obtained [16]:

$$\overline{Y} = \frac{3}{Bi}\left[\exp(Bi^2\tau) \cdot \operatorname{erfc}\left(Bi\sqrt{\tau}\right) - 1 + \frac{2}{\sqrt{\pi}}Bi\sqrt{\tau}\right] = \frac{3}{Bi} \cdot f_2\left(Bi\sqrt{\tau}\right) \tag{21}$$

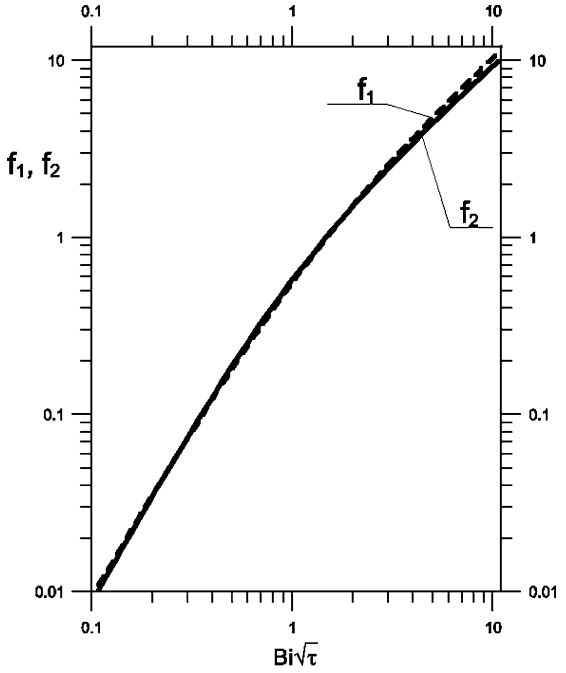

Fig. 2. Comparison of the functions f_1 and f_2.

A comparison of the function f_1 and f_2 is shown in Fig. 2. It is evident that for $Bi\sqrt{\tau} < 10$ these two functions are almost identical. Futhermore, for the particular case of $Bi \to \infty$, Eq. (12) is approximately reduced to the well known asymptotically exact form [15]:

$$\overline{Y} = \frac{6}{\sqrt{\pi}}\sqrt{\tau} \tag{22}$$

3. Development of the model of nonisothermal adsorption

The following assumptions are made in this analysis:

- There are no temperature gradients inside the particle and the heat transfer resistance is contributed by the film surrounding the particle.
- The adsorption equilibrium is described by a Freundlich isotherm and the temperature changes have negligible effect on the equilibrium.
- Mass transfer inside the particle is attributed to pore diffusion.
- The diffusion coefficient, heat capacity and heat of sorption are independent of temperature and concentration.
- Chilton–Colburn analogy is applicable.

Based on these assumptions the heat balance of the particle is described by the equation:

$$\frac{4}{3}\pi R_p^3 \rho_p \Delta H \frac{d\bar{q}_m}{dt} = 4\pi R_p^2 h(T - T_b) + \frac{4}{3}\pi R_p^3 \rho_p c_p \frac{dT}{dt} \tag{23}$$

From Chilton–Colburn analogy we have $j_H = j_D$ and therefore taking into account the definitions of the heat and mass factors one obtains:

$$\frac{h}{u\rho_g c_g} Pr^{2/3} = \frac{k_g}{u} Sc^{2/3} \tag{24}$$

and therefore

$$\frac{h}{k_g} = \rho_g c_g \psi \tag{25}$$

where

$$\psi = \left(\frac{Sc}{Pr}\right)^{2/3} \tag{26}$$

Defining the dimensionless particle temperature as

$$\theta = \frac{T - T_0}{T_0} \tag{27}$$

the heat balance can be rewritten in dimensionless form as

$$\zeta \frac{d\overline{Y}}{d\tau} = 3Bi\psi(\theta - \theta_b) + \frac{1}{\sigma}\frac{d\theta}{d\tau} \tag{28}$$

where

$$\zeta = \frac{\Delta H \cdot C_b}{\rho_g c_g T_0} = \frac{\Delta T_{ad}}{T_0} \tag{29}$$

$$\sigma = \frac{\rho_g c_g}{\rho_p c_p} \lambda \tag{30}$$

$$\theta_b = \frac{T_b - T_0}{T_0} \tag{31}$$

and ΔT_{ad} $(=\Delta H \cdot C_b/(\rho_g c_g))$ is the adiabatic temperature increase.

Combining Eqs. (5), (13), (28) one obtains:

$$\frac{3Bi \cdot \zeta}{\gamma\sqrt{1+\delta\tau}} = 3Bi\psi(\theta - \theta_b) + \frac{1}{\sigma}\frac{d\theta}{d\tau} \tag{32}$$

The analytical solution of the above differential equation with the initial condition

$$\tau = 0, \quad \theta = 0 \tag{33}$$

is developed in Appendix A and is given by the equation:

$$\theta = \theta_b + \frac{\dfrac{2\zeta\sqrt{\eta}}{\gamma\psi \cdot \exp(\eta)} \displaystyle\int_{\sqrt{\eta}}^{\sqrt{\eta(1+\delta\tau)}} \exp(z^2)\,dz - \theta_b}{\exp(\eta\delta\tau)} \tag{34}$$

where

$$\eta = \frac{3\sigma Bi\psi}{\delta} \tag{35}$$

The integral in Eq. (34) can be calculated by expanding the integrand into series and subsequent integration term by term:

$$\int \exp(x^2)\,dx = \sum_{k=0}^{\infty} \frac{x^{2k+1}}{(2k+1)k!} \tag{36}$$

4. The influence of the isotherm nonlinearity and film mass-transfer coefficient on the temperature uptake curves

For a given set of the parameters ν, Bi, σ, ψ, ζ and θ_b, Eq. (34) defines a temperature uptake curve. The Freundlich exponent ν is a measure of the isotherm nonlinearity. For systems of practical importance the isotherm is favourable and ν takes values in the interval $(0 < \nu < 1)$. The limiting values correspond to the important theoretical cases of irreversible and linear isotherm.

The mass-Biot number characterises the relation between the external and internal mass-transfer resistances and increases with increasing film mass-transfer coefficient or decreasing intraparticle diffusivity. It is important to note that the heat Biot number is zero (negligible intraparticle heat-transfer resistances). For most systems of practical importance the mass-Biot number is usually many orders of magnitude greater than the heat Biot number.

Parameter σ characterises the relation between the mass and heat capacities of the two phases. In most cases $\sigma \gg 1$. In the case of linear systems, σ is constant while for nonlinear systems it is a function of the fluid phase concentration.

Parameter ζ is proportional to the heat of adsorption. In Figs. 3–7, the quotient of the dimensionless particle temperature θ and the parameter ζ was used as dependent variable.

In Figs. 3–5 the temperature uptake curves in the form $\theta/\zeta = f(\tau)$ for various values of the parameters ν, Bi and σ are shown. The parameters θ_b and ψ were kept constant ($\theta_b = 0$ and $\psi = 1$). Figs. 3 and 4 show the influence of the isotherm nonlinearity and Biot number on the temperature uptake curves. With decreasing Freundlich exponent ν the heat effects are greater due to the increasing mass-transfer rate. With increasing Biot number however, the heat effects are becoming smaller. This is due to the fact that as a result of the Chilton and Colburn analogy, an increase in the film mass-transfer coefficient leads to an increase of the film heat transfer coefficient. Since the heat-transfer resistances are entirely located in the film surrounding the particle, while the mass-transfer resistances are located both in the film and inside the particle, a decrease in the film resistances has a greater effect on the overall heat-transfer rate rather than on the overall mass-transfer rate. As a result, with increasing mass-Biot number the time needed to achieve the temperature maximum is decreasing (Figs. 3 and 4). It is interesting to note that with increasing Biot numbers the influence of the isotherm nonlinearity becomes smaller.

In Fig. 5 the effect of the parameter σ on the temperature uptake curves is illustrated. With increasing σ, the heat effects become greater. This is expected, since σ is

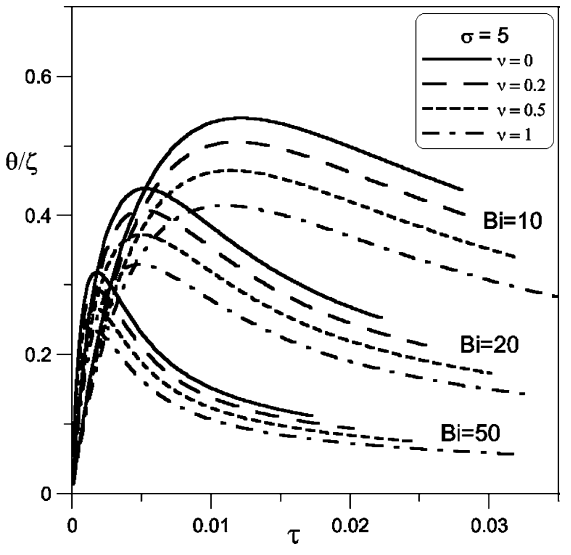

Fig. 3. Temperature uptake curves for $\sigma = 5$ and different values of ν and Bi.

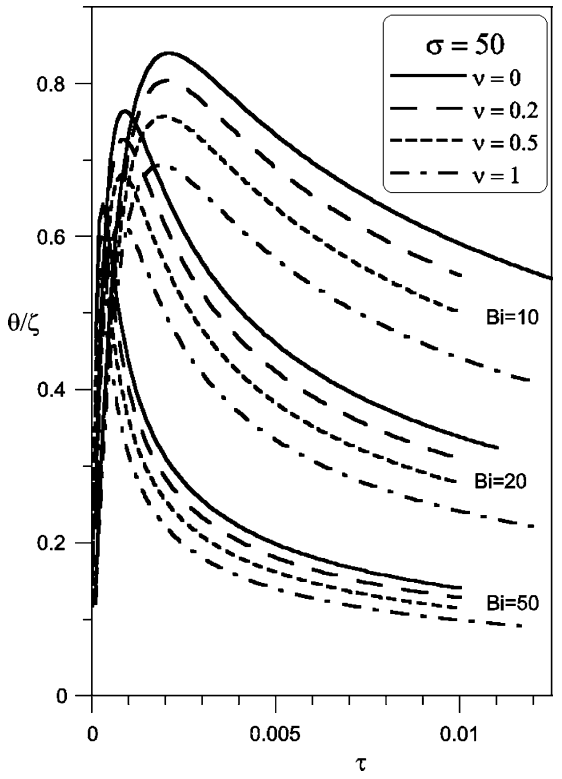

Fig. 4. Temperature uptake curves for $\sigma = 50$ and different values of v and Bi.

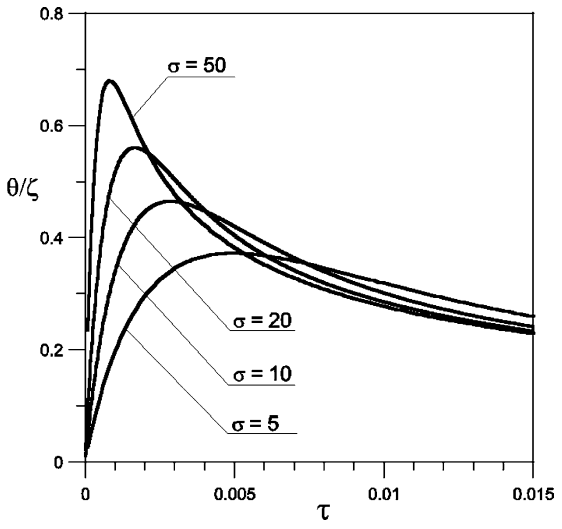

Fig. 5. Temperature uptake curves for $v = 0.5$, $Bi = 20$ and different values of σ.

proportional to the mass capacity and inversely proportional to the heat capacity of the solid phase.

In Fig. 6, the influence of the fluid-phase initial temperature (parameter θ_b/ζ) is illustrated. With decreasing

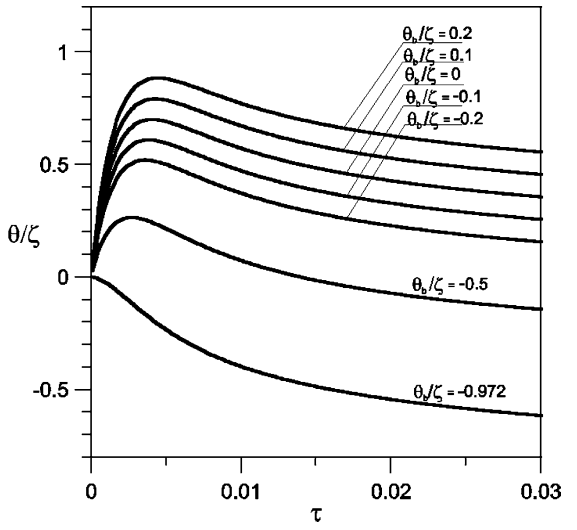

Fig. 6. Temperature uptake curves for $v = 0.2$, $Bi = 10$, $\sigma = 20$, $\psi = 1$ and different values of θ_b.

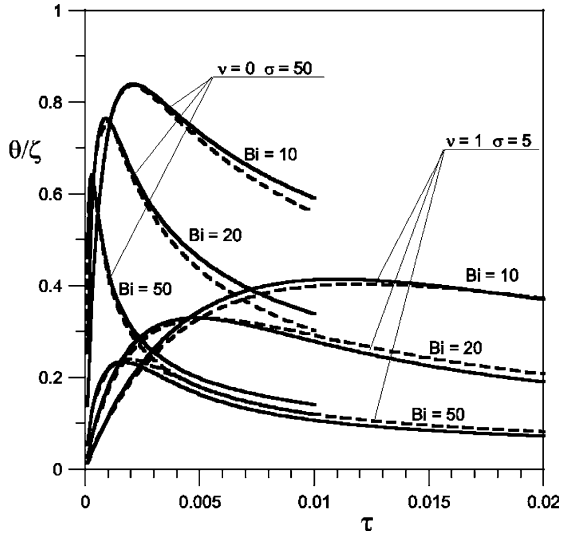

Fig. 7. Comparison of the temperature uptake curves obtained from the new model (Eq. (34)—solid lines) and the exact models (dashed lines) for linear and irreversible isotherms.

initial fluid-phase temperature, the maximum temperature and the time needed to achieve it decrease. A criterium for the existence of a temperature maximum will be discussed in Section 5.

A comparison of the temperature uptake curves resulting from the approximate model and the solutions for the linear and irreversible isotherms is shown in Fig. 7.

In the case of an irreversible isotherm, the mass-transfer rate is given by:

$$\frac{d\overline{Y}}{d\tau} = \frac{3(1-\overline{Y})^{1/3}}{1-(1-\overline{Y})^{1/3}\left(1-\frac{1}{Bi}\right)} \tag{37}$$

Therefore

$$\overline{Y} = 1 - \frac{1}{\left(1-\frac{1}{Bi}\right)^3}\left\langle \frac{1}{2} + \cos\left\{\frac{\pi}{3} + \frac{1}{3}\cdot \arccos\left[\left(1-\frac{1}{Bi}\right)^2\left(2+\frac{4}{Bi}-12\tau\right)-1\right]\right\}\right\rangle^3 \tag{38}$$

Taking into account the above relations and Eq. (28), an ordinary differential equation is obtained which with the condition (33) was integrated numerically.

For a linear isotherm the solution for the temperature uptake curve is given by [7]

$$\theta = \frac{1}{\psi+\frac{Bi}{3\sigma}}\cdot\left[\exp(Bi^2\tau)\cdot \operatorname{erfc}\left(Bi\sqrt{\tau}\right) - \exp(-3Bi\sigma\psi\tau) + \frac{2}{\sqrt{\pi}}\sqrt{\frac{Bi}{3\sigma\psi}}\exp(-3Bi\sigma\psi\tau)\cdot\int_0^{\sqrt{3Bi\sigma\psi\tau}}\exp(z^2)\,dz\right] \tag{39}$$

We observe that at the limiting cases, the approximate model agrees very well with the exact models.

5. Maximum particle temperature

All temperature uptake curves shown in the figures have a maximum. In the initial stages of the process, the rate of adsorption and therefore the rate of heat generation are high. On the other hand the heat transfer rate is low resulting in an increase in particle's temperature. When at a later stage of the process, the rates of heat generation and heat transfer become equal, the particle temperature achieves a maximum. In the last stage of the process the particle temperature decreases asymptotically to the bulk temperature.

The time τ_m needed to achieve the maximum temperature can be calculated using the equation

$$\int_{\sqrt{\eta}}^{\sqrt{\eta p}}\exp(z^2)\,dz = \frac{1}{2\sqrt{\eta}}\left[\frac{\exp(\eta p)}{\sqrt{p}} + \exp(\eta)\cdot\frac{\gamma\psi}{\zeta}\theta_b\right] \tag{40}$$

where (see Appendix B)

$$p = 1 + \delta\tau_m \tag{41}$$

The above Eq. (41) can be formally written as

$$p = f(\eta, \theta_b') \tag{42}$$

where

$$\theta_b' = \frac{\gamma\psi}{\zeta}\theta_b \tag{43}$$

The function $p = f(\eta, \theta_b')$ is shown in Fig. 8.

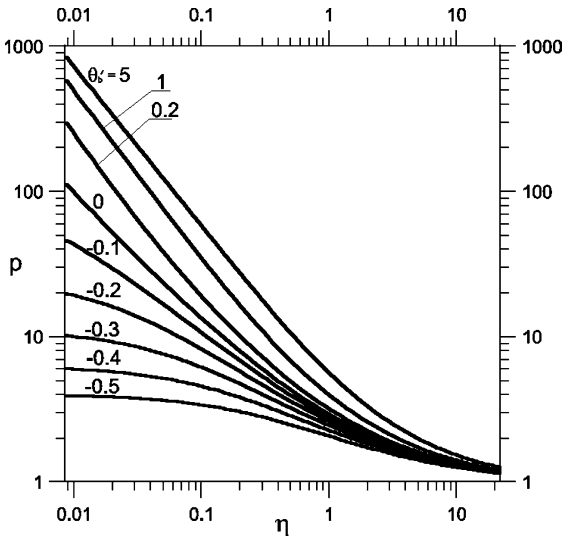

Fig. 8. The dependency of p on η for various values of θ_b'.

The maximum temperature can be calculated using the equation (see Appendix B):

$$\theta_m = \theta_b + \frac{\zeta}{\gamma\psi}\frac{1}{\sqrt{p}} \tag{44}$$

The above equation results from Eq. (32) upon substitution $d\theta/d\tau = 0$.

The calculation of the maximum particle temperature and the time τ_m for known values of the parameters v, Bi, σ, ψ, ζ and θ_b is based on the following algorithm:

- Calculate β and γ using Eqs. (10) and (11).
- Calculate δ using Eq. (14) and η using Eq. (35).
- Determine θ_b' from Eq. (43).
- From Fig. 8 find p.
- Calculate τ_m using Eq. (41).
- Calculate the dimensionless temperature increase using Eq. (44).
- The maximum increase of the temperature is then given by

$$T_m - T_0 = T_0\theta_m \tag{45}$$

The influence of parameter θ_b on the temperature uptake curves has been discussed in the previous section (Fig. 6). For a critical value of this parameter no temperature maximum is observed. This situation arises when the rate of heat generation at the beginning of the process is smaller or equal to the rate of heat transfer. In the critical case when the two rates are equal we have ($\tau = 0$, $\overline{Y} = 0$, and $d\theta/d\tau = 0$). Therefore, from Eqs. (5) and (28) we have

$$\frac{\zeta}{\gamma\psi} = \theta - \theta_{b,crit} \tag{46}$$

At $\tau = 0$, the dimensionless temperature is zero ($\theta = 0$), therefore

$$\theta_{b,crit} = -\frac{\zeta}{\gamma\psi} \tag{47}$$

Eq. (47) can be also derived from Eq. (44) by substituting $\tau_m = 0$ and $\theta_m = 0$.

If the heat effects are negligible then $\zeta = 0$ and $\theta_{b,crit} = 0$. In this case the temperature uptake curve monotonically increases or decreases depending on the value of θ_b.

The lower curve in Fig. 6 is an example of the critical case where Eq. (47) is applicable. We observe that the temperature uptake curve is monotonous.

6. Comparison with experiment

The presented model has been used to predict the temperature uptake curves using the data presented by Bowen and Rimmer [9] for the adsorption of water vapour on alumina at 30 °C and at a gas-phase velocity of 0.36 m/s. The equilibrium data [9] were used to calculate the parameters of the Freundlich isotherm:

$$q_m = K_F p^v \tag{48}$$

where $p = RH \cdot p_s$. The parameters K_F and v are functions of the temperature (Do [17]):

$$K_F = K_0 \exp\left(-\frac{ART}{E_0}\right) \tag{49}$$

$$v = \frac{RT}{E_0} \tag{50}$$

where A is a constant in the Clausius–Clapeyron equation:

$$\ln p_s = A - \frac{B}{T} \tag{51}$$

In the temperature interval 30–42 °C, the constants of Eq. (51) for water vapour are $A = 25.654$, $B = 5242.2$. The so obtained values at $T = 30$ °C and $RH < 0.5$ were $K_F = 0.002636$, $v = 0.5064$. The resulting values for the parameters K_0 and E_0 are $K_0 = 1152$ and $E_0 = 4975$ J/mol. In Fig. 9, the experimental equilibrium data and the Freundlich isotherm are presented. It is obvious that the Freundlich isotherm describes well the equilibrium.

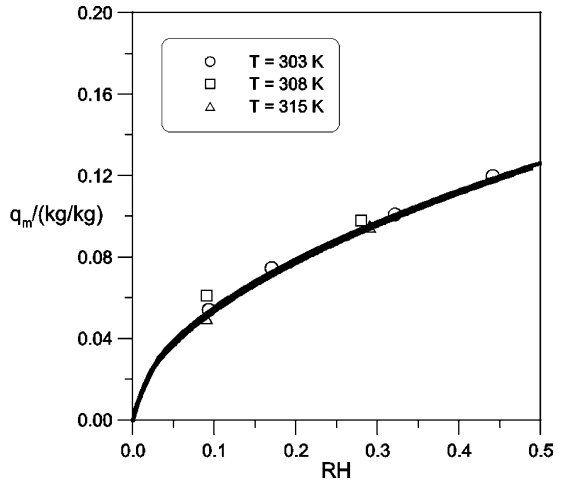

Fig. 9. Freundlich equation equilibrium fitting to the experimental data [9] for $RH < 0.5$.

The necessary for the computations data are [7,9]: $R_p = 0.00109$ m, $\rho_p = 1154$ kg/m^3, $c_p = 840$ J/kg K, $\Delta H = 2{,}720{,}000$ J/kg, $k_g = 0.071$ m/s.

The data for the gas-phase (air) are $\rho_g = 1.13$ kg/m^3, $c_g = 1013$ J/kg K. The diffusion coefficient of water vapour in air at 0 °C is 22.0×10^{-6} m^2/s [18]. Therefore at 30 °C we have $D = 22.0 \times 10^{-6}\ (303/273)^{1.7} = 26 \times 10^{-6}$ m^2/s.

Three experimental series were used each for a different relative humidity. The parameters for each one are shown in Table 1. In all cases $\theta_b = 0$. Two values of the effective pore diffusivity were used. The one resulting from the approximate expression $D_{p1} = D/10 = 2.6 \times 10^{-6}$ m^2/s. The other one $D_{p2} = 3.6 \times 10^{-6}$ m^2/s was taken from [9]. The resulting Biot numbers are 30.0 and 21.5.

In the case of the system air–water vapour, the Prandtl and Schmidt numbers are approximately equal and therefore (Eq. (26)) $\psi = 1$. In Fig. 10 a comparison of the experimental results and the model predictions are shown. In the case of $RH = 0.096$, the model predictions agree very well with the experimental results. For $RH = 0.299$ the agreement is reasonable although an underestimation of the maximum temperature is observed. For $RH = 0.514$, the differences are too large and the model seems to be inadequate. This should be attributed to various factors such as:

Table 1
Model parameters

RH	C_b (kg/m^3)	q_{mb} (kg/kg)	λ	ΔT_{ad} (K)	σ	$(\partial q_m/\partial T)_p$	α'	β'
0.096	0.00291	0.0552	21910	6.9	25.9	−0.00080	2310	2.59
0.299	0.00906	0.0982	12505	21.5	14.8	−0.00142	1319	4.60
0.514	0.01557	0.1292	9570	37.0	11.3	−0.00187	1009	6.05

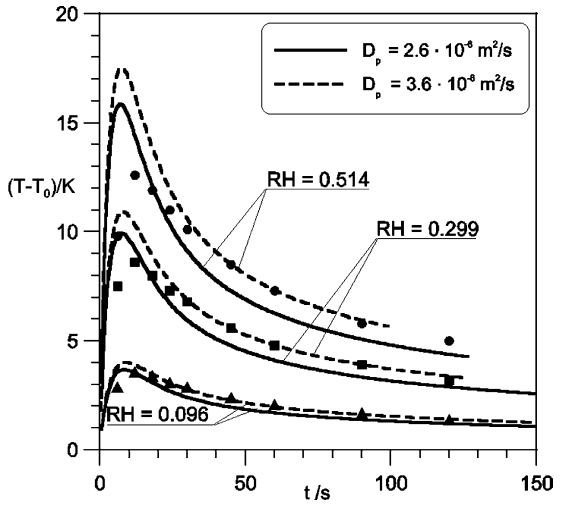

Fig. 10. Comparison of experimental results [9] (points) and the predictions of the approximate model (lines).

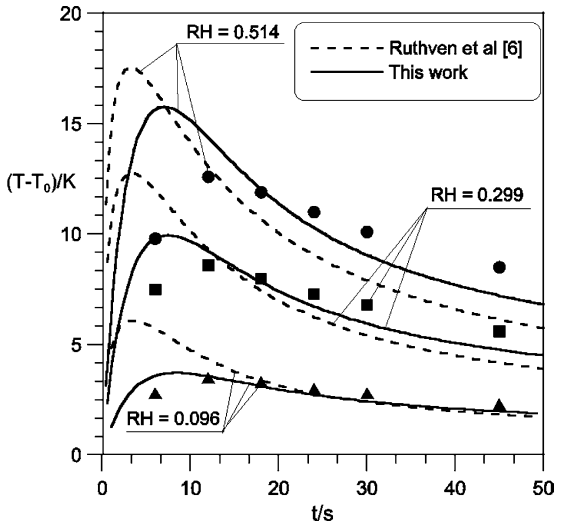

Fig. 11. Comparison of the new model (Eq. (34)—solid line) with the model [6] (dashed line) and the experimental results for $D_p = 2.6 \times 10^{-6}$ m^2/s.

(a) The isotherm (Eq. (48)) is based on data for RH < 0.5.
(b) The temperature increases and their influence on the equilibrium are significant. This is in agreement with the findings of Hills [7] who states that for temperature increases exceeding 10 K the assumption of negligible influence of the heat effects on the equilibrium is no longer applicable. As will be shown later however, an iterational computation scheme improves substantially the accuracy of the model.

In Fig. 11 a comparison of the predictions of the new model (Eq. (34)) with the model (Eqs. (1)–(4)) by Ruthven et al. [6] is presented. The calculation of the parameter β' requires the value of the derivative $(\partial q_m/\partial T)_p$. From Eqs. (48)–(51) it can be readily shown that

$$\left(\frac{\partial q_m}{\partial T}\right)_p = -\frac{RB}{E_0\, T}\cdot q_m \qquad (52)$$

The average value of the derivative was found for $q_m = q_{mb}/2$ and is given in Table 1 with the values of the parameters α' and β'.

It is obvious from Fig. 11 that Ruthven's et al. [6] model significantly deviates from the experimental data at the initial stage of the process. This is a consequence of the assumption that the external mass-transfer resistances are negligible. At the initial stages of the process however the intra-particle mass-transfer rate is large and the external mass-transfer resistances are rate controlling. Furthermore, the predicted by the model (Eqs. (1)–(4)) maximum temperature rise is significantly overestimated. On the other hand, the predictions of the new model (Eq. (34)) agree well with the experimental data. This shows that the assumption that the isotherm parameters are temperature independent leads to smaller errors than the assumption of negligible external mass-transfer resistances. This is in agreement with the findings by Hills [7].

In Fig. 12 a comparison of the predictions of two models (Hills [7] and Eq. (34)) is shown. The model presented by Hills [7] is based on a linear isotherm

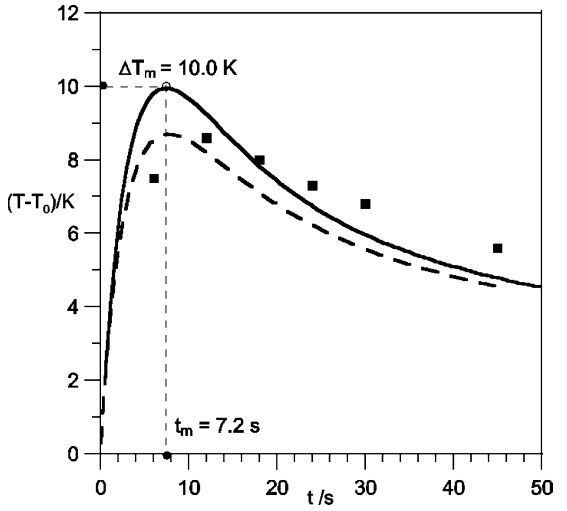

Fig. 12. Comparison of the new model (Eq. (34)—solid line) with the model [7] (dashed line) and the experimental results for RH = 0.299 and $D_p = 2.6 \times 10^{-6}$ m^2/s.

assumption. The values of the parameters ΔT_m and t_m were calculated as follows:

- From Eqs. (10) and (11) the parameters β and γ were calculated $\beta = 0.522$, $\gamma = 1.077$.
- From Eqs. (14) and (35) the parameters δ and η were calculated:

$$\delta = 6 \cdot 0.522 \cdot (30)^2/(1.077)^2 = 2430$$
$$\eta = 3 \cdot 15.1 \cdot 30 \cdot 1/2430 = 0.559$$

- Using the values of η and for $\theta'_b = 0$, the parameter p was found from Fig. 8; $p \cong 4.0$.
- The parameter τ_m was found from Eq. (41): $\tau_m = 0.00123$. Therefore (Eq. (7)):

$$t_m = 12,790 \cdot (0.00109)^2 \cdot 0.00123/(2.6 \times 10^{-6}) = 7.2 \text{ s}$$

- The parameter ζ was calculated:

$$\zeta = 21.5/303 = 0.0709$$

- The maximum dimensionless temperature was found:

$$\theta_m = 0 + 0.0709/\left(1.077 \cdot 1 \cdot \sqrt{4.0}\right) = 0.0329$$

- The temperature increase was found:

$$\Delta T_m = 0.0329 \cdot 303 = 10.0 \text{ K}$$

- The critical bulk temperature for the existence of a maximum in the temperature uptake curve was found:

$$\theta_{b,crit} = -0.0709/(1.077 \cdot 1) = -0.0658$$
$$T_{crit} - T_0 = -0.0658 \cdot 303 = -19.9 \text{ K}$$

Therefore for bulk temperatures below $30 - 19.9 = 10.1$ °C no maximum exists.

In the presented analysis, the calculation of the temperature uptake curve based on Eq. (34) was made using the values of the isotherm parameters for the initial temperature T_0. The accuracy of the model improves if the parameters are determined at the average temperature $T_0 + 0.5 \cdot \Delta T_m$. In Fig. 13 a comparison of the predictions of the model (Eq. (34)) using the values of the parameters for the initial temperature $T_0 = 30$ °C and the average temperature $T_0 + 0.5 \cdot \Delta T_m = 30 + 0.5 \cdot 15.8 = 37.9$ °C is presented. We observe that the application of the corrected values of the parameters improves the accuracy of the model and the predicted temperature uptake curve is in better agreement with the experimental data. It is therefore recommended that the model (Eq. (34)) is applied initially using the values of the parameters for $T = T_0$ to calculate ΔT_m and subsequently is applied using the values of the parameters for $T = T_0 + 0.5 \cdot \Delta T_m$.

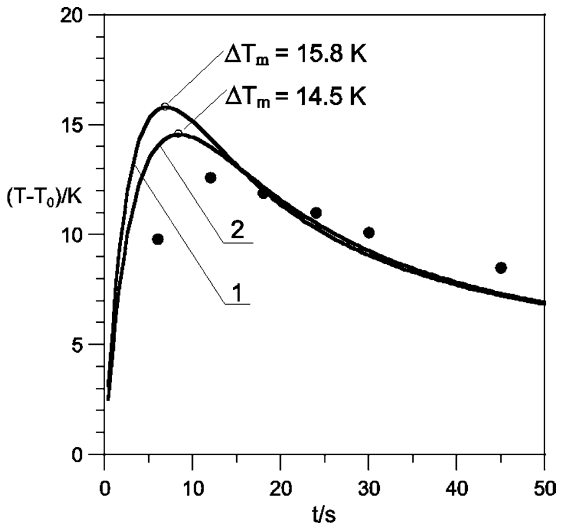

Fig. 13. Iterative computation of the temperature uptake curve. RH = 0.514, $D_p = 2.6 \times 10^{-6}$ m^2/s. Line 1: parameters calculated for initial temperature. Line 2: parameters calculated for average temperature.

7. Conclusions

The presented results lead to the following conclusions:

1. The application of the kinetic equation (5) leads to a new model of nonisothermal adsorption which is analytically integrable. The new model is applicable to systems with a nonlinear isotherm and accounts for both intraparticle (pore diffusion) and film mass-transfer resistances as well as film heat transfer resistances. This new model is the only currently available model, which is analytically integrable for a nonlinear isotherm.
2. The new model has been applied to describe the influence of the isotherm nonlinearity and the Biot number on the temperature uptake curves. It is shown that the heat effects are increasing with increasing isotherm nonlinearity.
3. The predictions of the new model agree well with the experimental results presented in [9] and with the predictions of the exact models for linear and irreversible isotherms.
4. A simple algorithm presented in this work allows the calculation of the maximum temperature and can be usefull in the assessment whether a process may be assumed isothermal.
5. The new model leads to a simple criterium for the existence of a maximum in the temperature uptake curve.

Appendix A. Analytical integration of Eq. (32)

Eq. (32) is transformed to give:

$$\frac{\exp(3\sigma Bi\psi\tau)}{\gamma\sqrt{1+\delta\tau}} = \frac{1}{3\sigma Bi}\frac{\mathrm{d}}{\mathrm{d}\tau}[(\theta-\theta_\mathrm{b})\exp(3\sigma Bi\psi\tau)] \tag{A.1}$$

Both sides of Eq. (A.1) are integrated with respect to time taking into account the initial condition Eq. (33):

$$\frac{3\sigma Bi}{\gamma} I = (\theta-\theta_\mathrm{b})\exp(3\sigma Bi\psi\tau) + \theta_\mathrm{b} \tag{A.2}$$

where

$$I = \int_0^\tau \frac{\exp(3\sigma Bi\psi\tau)}{\sqrt{1+\delta\tau}}\,\mathrm{d}\tau \tag{A.3}$$

The integral is calculated:

$$I = \frac{2\sqrt{\eta}}{\eta\delta\cdot\exp(\eta)}\int_{\sqrt{\eta}}^{\sqrt{\eta(1+\delta\tau)}} \exp(z^2)\,\mathrm{d}z \tag{A.4}$$

Appendix B. Determination of the maximum of the temperature uptake curve

Eq. (34) was differentiated with respect to time and set equal to zero. Taking into account that:

$$\begin{aligned}&\frac{\mathrm{d}}{\mathrm{d}\tau}\int_{\sqrt{\eta}}^{\sqrt{\eta(1+\delta\tau)}} \exp(z^2)\,\mathrm{d}z \\ &= \frac{\mathrm{d}\left[\sqrt{\eta(1+\delta\tau)}\right]}{\mathrm{d}\tau}\cdot\frac{\mathrm{d}}{\mathrm{d}\left[\sqrt{\eta(1+\delta\tau)}\right]}\int_{\sqrt{\eta}}^{\sqrt{\eta(1+\delta\tau)}} \exp(z^2)\,\mathrm{d}z \\ &= \frac{\eta\delta}{2\sqrt{\eta(1+\delta\tau)}}\cdot\exp[\eta(1+\delta\tau)]\end{aligned} \tag{B.1}$$

we obtain

$$\begin{aligned}&\int_{\sqrt{\eta}}^{\sqrt{\eta(1+\delta\tau_\mathrm{m})}} \exp(z^2)\,\mathrm{d}z \\ &= \frac{1}{2\sqrt{\eta}}\left\{\frac{\exp[\eta(1+\delta\tau_\mathrm{m})]}{\sqrt{1+\delta\tau_\mathrm{m}}} + \exp(\eta)\cdot\frac{\gamma\psi}{\zeta}\theta_\mathrm{b}\right\}\end{aligned} \tag{B.2}$$

Upon substitution of Eq. (B.2) to Eq. (34) we obtain

$$\theta_\mathrm{m} = \theta_\mathrm{b} + \frac{\zeta}{\gamma\psi}\frac{1}{\sqrt{1+\delta\tau_\mathrm{m}}} \tag{B.3}$$

References

[1] W.J. Thomas, B. Crittenden, Adsorption Technology & Design, Butterworth-Heinemann, 1998, pp. 187–239.

[2] D.M. Ruthven, S. Farooq, K.S. Knaebel, Pressure Swing Adsorption, VCH Publishers Inc., 1994, pp. 221–264.

[3] K. Kupiec, J. Rakoczy, R. Mirek, A. Georgiou, Ł. Zieliński, Determination and Analysis of Experimental Breakthrough Curves for Ethanol Dehydration by Vapour Adsorption on Zeolites, Inzynieria Chemiczna i Procesowa (Chemical and Process Engineering) 24 (2003) 293–310 (in Polish).

[4] D.M. Ruthven, L.-K. Lee, Kinetics of nonisothermal sorption: System with bed diffusion control, AIChE Journal 27 (1981) 654–663.

[5] R. Haul, H. Stremming, Nonisothermal sorption kinetics in porous adsorbents, Journal of Colloid and Interface Science 97 (1984) 349–355.

[6] D.M. Ruthven, L.-K. Lee, H. Yucel, Kinetics of non-isothermal sorption in molecular sieve crystals, AIChE Journal 26 (1980) 16–23.

[7] J.H. Hills, Non-isothermal adsorption in a pellet, Chemical Engineering Science 46 (1991) 69–74.

[8] A. Brunovska, V. Hlavacek, J. Ilavsky, J. Valtyni, An analysis of a nonisothermal one-component sorption in a single adsorbent particle, Chemical Engineering Science 33 (1978) 1385–1391.

[9] J.H. Bowen, P.G. Rimmer, The prediction of non-isothermal sorption in single pellets using the quadratic driving force equation, Chemical Engineering Journal 6 (1973) 145–156.

[10] T. Vermeulen, Theory of irreversible and constant-pattern solid diffusion, Industrial and Engineering Chemistry 45 (1953) 1664.

[11] G.V. Bhaskar, D.D. Do, A simple solution for nonisothermal adsorption in a single pellet, Chemical Engineering Science 44 (1989) 1215–1219.

[12] K. Kupiec, Rate of Mass Transfer for adsorption with external diffusion resistance. nonlinear adsorption systems, Inzynieria Chemiczna i Procesowa (Chemical and Process Engineering) 18 (1997) 289–307 (in Polish).

[13] A. Georgiou, K. Kupiec, Nonlinear driving force approximation for intraparticle mass transfer in adsorption processes. Nonlinear isotherm systems with macropore diffusion control, Chemical Engineering Journal 92 (2003) 185–191.

[14] A. Georgiou, Asymptotically exact driving force approximation for intraparticle mass transfer in diffusion and adsorption processes. Nonlinear isotherm systems with macropore diffusion, Chemical Engineering Science 59 (2004) 3591–3600.

[15] M. Suzuki, Adsorption Engineering, Kodansha, Elsevier, 1990, pp. 95–124.

[16] J. Crank, The Mathematics of Diffusion, Oxford University Press, 1956, p. 34.

[17] D.D. Do, Adsorption Analysis: Equilibria and Kinetics, Imperial College Press, 1998, pp. 50–57.

[18] R.H. Perry, D.W. Green, J.O. Maloney, Perry's Chemical Engineers' Handbook, McGraw-Hill, 1997, pp. 2–329.